

Direct genetic demonstration of G α 13 coupling to the orphan G protein-coupled receptor G2A leading to RhoA-dependent actin rearrangement

Janusz H. S. Kabarowski*, Jamison D. Feramisco*, Lu Q. Le*, Jennifer L. Gu[†], Shih-Wen Luoh**[‡], Melvin I. Simon[†], and Owen N. Witte*^{§¶}

*Department of Microbiology, Immunology, and Molecular Genetics and [§]Howard Hughes Medical Institute, University of California, Los Angeles, CA 90095-1662; and [†]Division of Biology, California Institute of Technology, Pasadena, CA 91125

Contributed by Owen N. Witte, August 22, 2000

G2A is an orphan G protein-coupled receptor (GPCR), expressed predominantly in T and B cells and homologous to a small group of GPCRs of unknown function expressed in lymphoid tissues. G2A is transcriptionally induced in response to diverse stimuli, and its ectopic expression suppresses transformation of B lymphoid precursors by BCR-ABL. G2A induces morphological transformation of NIH 3T3 fibroblasts. Microinjection of constructs encoding G2A into Swiss 3T3 fibroblasts induces actin reorganization into stress fibers that depends on RhoA, but not CDC42 or RAC. G2A elicits RhoA-dependent transcriptional activation of serum response factor. Direct evaluation of RhoA activity demonstrates elevated levels of RhoA-GTP in G2A-expressing cells. Microinjection of embryonic fibroblasts derived from various G α knockout mice establishes a requirement for G α 13 but not G α 12 or G α q/11 in G2A-induced actin rearrangement. In conclusion, G2A represents a family of GPCRs expressed in lymphocytes that may link diverse stimuli to cytoskeletal reorganization and transcriptional activation through a pathway involving G α 13 and RhoA.

The seven transmembrane spanning G protein-coupled receptors (GPCRs) constitute the largest family of cell-surface receptors, controlling diverse biological processes. Ligand binding to GPCRs elicits activation of signaling pathways via associated heterotrimeric G proteins comprising α , β , and γ subunits. Both GTP-bound α and free $\beta\gamma$ components mediate signaling events through their interaction with effector molecules, leading to an appropriate physiological response. Biological/biochemical responses to activation of a GPCR are determined primarily by the nature of the G α subunits to which it is coupled, and this property cannot be predicted by primary sequence analysis of newly discovered GPCRs (1). A key objective in the study of an orphan GPCR is to define its G α coupling profile. Direct experimental approaches such as photolabeling of G α subunits with radiolabeled GTP analogues (2) are limited in their application to the study of GPCRs in the absence of a defined ligand/agonist. However, signaling events downstream of many G α subunits are well defined, and their analysis can serve as surrogate assays of G α coupling profiles. Indeed, the biochemical/signaling properties of GPCRs are most often recapitulated in heterologous cell types (3, 4), and cell lines in which the spectrum of expressed G α subunits are defined can serve as systems in which to study the primary signal transduction and biological characteristics of orphan GPCRs (5).

We previously have reported the identification of a novel GPCR, G2A, expressed predominantly in B and T lymphoid cells (6). G2A is homologous to a small number of orphan GPCRs of unknown function expressed in lymphoid tissues, among which TDAG8 is most closely related (7). The genes encoding G2A and TDAG8 both map to chromosome 14q31–32.1, a region in which abnormalities frequently are found in T cell leukemias and lymphomas (6, 8).

G2A is transcriptionally induced in B lymphocytes after antigen receptor crosslinking and in pre-B lymphocytes by the BCR-ABL tyrosine kinase oncogene. Interestingly, although transcriptional induction of G2A is associated with proliferative responses, its ectopic expression inhibits transformation of B cell precursors by BCR-ABL (6). We addressed the question of what mechanisms are involved in these biological effects by conducting studies aimed at defining signal transduction events downstream of G2A and their G α specificity.

In light of our previous observations demonstrating that ectopic expression of G2A is counterselected in fibroblasts and B lymphoid precursors (6), an experimental approach was used in which the potential for biological selection was avoided. Transient biochemical assays and microinjection of constructs encoding G2A into Swiss 3T3 fibroblasts and embryonic fibroblasts derived from G α knockout mice (G α KO MEFs) delineate a signaling pathway downstream of G2A to RhoA activation via G α 13 leading to actin rearrangement and serum response factor (SRF)-dependent transcriptional activation. Taken together, these observations suggest that G2A expression and transcriptional induction may play a role in the integration of proliferative and/or differentiative signals with cytoskeletal reorganization.

Materials and Methods

Materials. Rhodamine-conjugated phalloidin and antivinculin mAb (VIN-11-5) were from Sigma. Aminomethylcoumarin-conjugated secondary anti-rabbit antibody was from Jackson ImmunoResearch. All other fluorescently conjugated secondary antibodies were from PharMingen. Anti-RhoA mAb was from Santa Cruz Biotechnology. Anti-G α 13 polyclonal antibody (AS 343) was provided by Karsten Spicher (Benjamin Franklin University, Berlin).

Cell Lines and Plasmids. Wild-type and G α KO MEFs were prepared and cultured from embryonic day 8.5 to 9.5 embryos as described (9). Swiss 3T3, NIH 3T3, 293T and G α KO MEFs (G α 13 KO, ref. 9; G α q/11 KO, ref. 10; and G α 12 KO, M.I.S., unpublished work) were cultured in DMEM/10% FCS.

Abbreviations: GPCR, G protein-coupled receptor; KO, knockout; MEF, mouse embryonic fibroblast; SRF, serum response factor; GFP, green fluorescent protein; MSCV, murine stem cell virus.

[‡]Present address: Division of Hematology and Oncology, University of Cincinnati College of Medicine, Cincinnati, OH 45267-0508.

[¶]To whom reprint requests should be addressed at: HHMI/UCLA, 675 Charles E. Young Drive South, Room 5-720, MRL Building, Los Angeles, CA 90095-1662. E-mail: owenw@microbio.ucla.edu.

The publication costs of this article were defrayed in part by page charge payment. This article must therefore be hereby marked "advertisement" in accordance with 18 U.S.C. §1734 solely to indicate this fact.

293T cells were transfected by the calcium phosphate precipitation technique. The glutathione *S*-transferase-rhotekin Rho binding domain construct was provided by Martin Schwartz (The Scripps Research Institute, La Jolla, CA). pEXV3 V12 RAS, N19 RhoA, N17 CDC42, and N17 RAC constructs were provided by Chris Marshall (Institute of Cancer Research, London). pRK5 mycC3T was provided by Alan Hall (University College, London).

Microinjection and Immunocytochemical Staining. Cells for microinjection were plated at a density of 10^4 /ml onto 13-mm acid-washed glass coverslips. Two days later, cells were serum starved for 16 h. Plasmids in 50 mM Hepes (pH 7.4), 40 mM NaCl were injected into nuclei by using an Ependorf semiautomated injector assembled on an inverted Zeiss Axiovert 10 microscope. Approximately 200–250 cells were microinjected on each coverslip and returned to the incubator for an additional 4 h or as indicated. Coverslips subsequently were rinsed once in PBS and fixed in 4% paraformaldehyde/PBS for 10 min at room temperature. Coverslips were washed in PBS and permeabilized by incubation with PBS, 0.2% Triton X-100 for 5 min at room temperature before incubation with 1:100 G α 13 antiserum, 1:100 9E10 mAb, or 1:100 antivinculin mAb in PBS, 0.15% Triton X-100, 25 mg/ml BSA at room temperature for 1 h in a humidified chamber. Coverslips were washed four times in PBS and incubated with rhodamine-conjugated goat anti-mouse secondary antibody (for vinculin), aminomethylcoumarin-conjugated goat anti-mouse secondary antibody (for MYC epitope-tagged Rho family GTPases), or aminomethylcoumarin-conjugated goat anti-rabbit secondary antibody (for G α 13) at 1:100 for 1 h at room temperature in a humidified chamber. Where appropriate, 0.2 μ g/ml rhodamine-conjugated phalloidin also was included. Coverslips were washed four times in PBS followed by one wash in H₂O and mounted by inversion onto 5 μ l Gelvatol mountant. Cells were examined on a Zeiss axiophot microscope with a Zeiss 40 \times 1.3 oil immersion objective. In all experiments, more than 90% of injected cells exhibited the described response.

SRF Luciferase Assays. NIH 3T3 cells were cotransfected with 0.2 μ g of the reporter plasmid pSRF-firefly luciferase (Stratagene), 0.2 μ g of pTK-*Renilla* luciferase (Promega), and 0.3 μ g of pEXV3 G2A or 0.3 μ g of pEXV3 green fluorescent protein (GFP), plus 0.2 μ g pRK5 mycC3T or 0.2 μ g pEXV3 GFP (totaling 0.9 μ g DNA) by the Superfect system (Life Technologies, Gaithersburg, MD). Twenty four hours later, cells were harvested, washed with PBS, and lysed in 200 μ l of Passive Lysis Buffer (Promega). Firefly and *Renilla* luciferase values were obtained by analyzing 10 μ l of lysate according to the standard protocol provided in the Dual Luciferase Assay Kit (Promega) in a Lumat LB 9501 luminometer (10-s count). Relative luciferase activity is represented as (firefly luciferase value/*Renilla* luciferase value) $\times 10^{-2}$.

Results

G2A Induces Morphological Alterations in Fibroblasts. Dramatic morphological alterations, including suppression of contact inhibition and reduced spreading, are readily apparent in NIH 3T3 fibroblasts less than 48 h after their infection with G2A-encoding retroviruses (Fig. 1A). G2A-expressing cells in subconfluent cultures appear elongated and tightly packed, with a significantly greater proportion detached and rounded. These morphological changes are quite distinct from those induced after infection with retroviruses encoding V12 RAS, which exhibit a more refractile morphology and focal organization (Fig. 1A). Suppression of contact inhibition of growth is even more apparent in confluent G2A-expressing cultures, which form tightly packed foci (Fig. 1B).

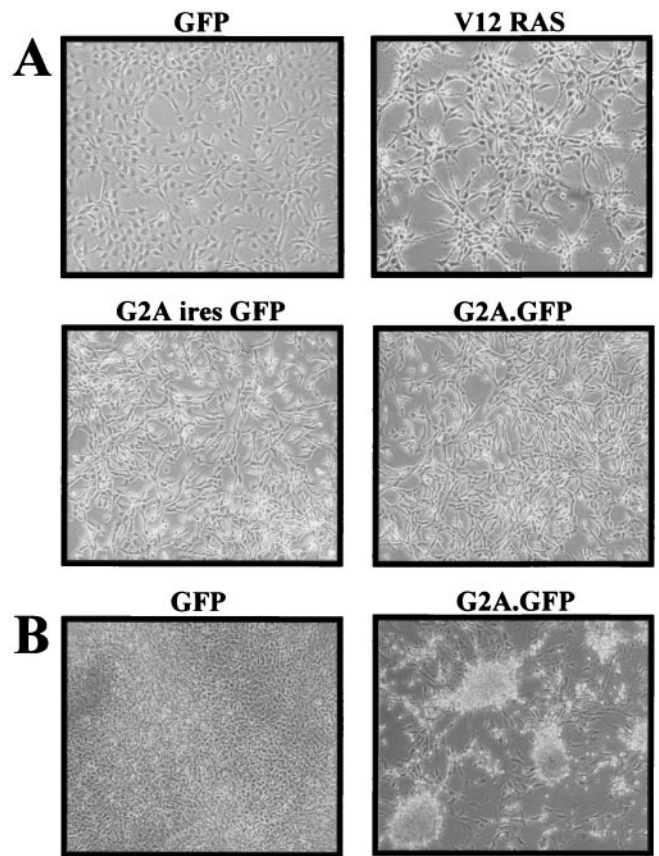


Fig. 1. G2A induces morphological alterations in NIH 3T3 cells. (A) NIH 3T3 cells were infected with the indicated retroviruses and cultured for an additional 36 h. All populations were more than 90% GFP-positive by FACS analysis. (B) NIH 3T3 cells infected with the indicated retroviruses were cultured for 7 days.

We speculated that the morphological changes induced by G2A may result from deregulation of mechanisms controlling cytoskeletal architecture. This prompted us to examine the involvement of Rho family GTPases, which relay signals from cell surface receptors including GPCRs, receptor tyrosine kinases, and integrins to the actin cytoskeleton (11, 12).

G2A Induces Assembly of Actin Stress Fibers in Swiss 3T3 Cells. To avoid prolonged expression of G2A during which biological adaptation and selection may contribute to the cellular phenotype, we used microinjection of Swiss 3T3 cells, a system in which acute regulation of expression is readily achieved in a cell type whose complement of expressed G α subunits is known (13). Initially, G2A encoding constructs to be used in these studies (pEXV3 G2A and pEXV3 G2A.GFP) were transfected into 293T cells to ensure expression of G2A and G2A.GFP proteins. Western blotting with affinity-purified rabbit antiserum raised against carboxyl-terminal sequences of G2A reveals proteins of expected size (data not shown).

Nuclear microinjection of pEXV3 G2A or pEXV3 G2A.GFP at 10 ng/ μ l into Swiss 3T3 cells elicited the formation of actin stress fibers and assembly of focal adhesion complexes (Fig. 2A). A construct encoding a nuclear GFP protein (pEXV3 GFP) was coinjected at 10 ng/ μ l in all experiments apart from those performed with G2A.GFP to identify productively injected cells. In this and all other experiments, approximately 200–250 cells were microinjected and all possible microscopic fields were examined. Both G2A

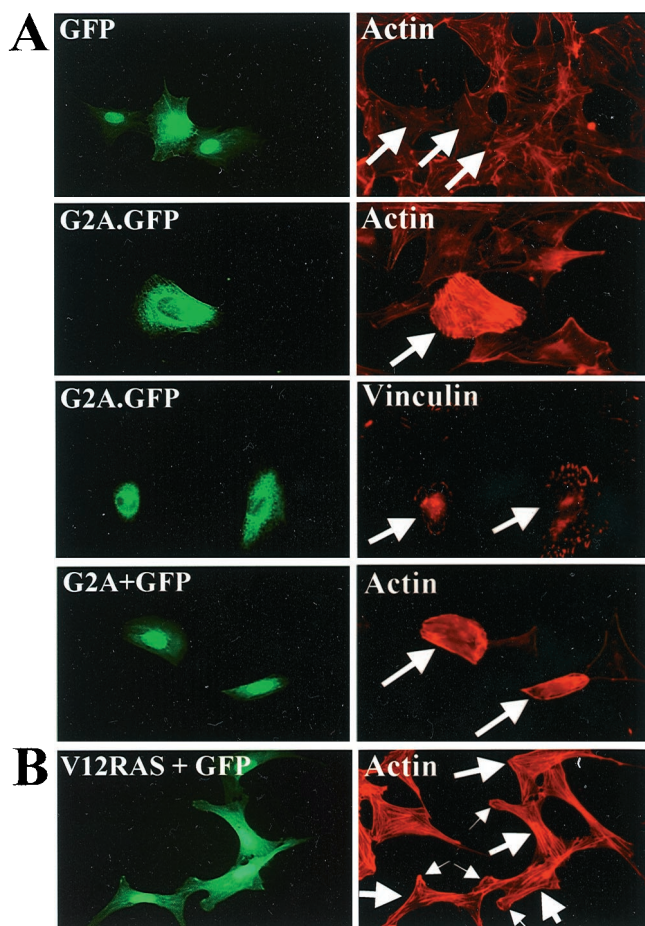


Fig. 2. (A) Microinjection of G2A induces stress fiber assembly in Swiss 3T3 cells. pEXV3 constructs encoding GFP, G2A.GFP, or G2A plus GFP were microinjected into nuclei of serum-starved Swiss 3T3 cells. Four hours later, cells were fixed and stained with rhodamine-conjugated phalloidin. In addition, pEXV3 G2A.GFP-injected cells were stained with a monoclonal antibody against Vinculin to visualize focal adhesion complexes. (B) Serum-starved Swiss 3T3 cells microinjected with a pEXV3 construct expressing V12 RAS were processed as in A. (Left) GFP fluorescence. (Right) Phalloidin-stained actin. Large arrows indicate injected cells. Small arrows in indicate lamellipodia in pEXV3 V12 RAS-injected cells.

and G2A.GFP consistently induce indistinguishable cytoskeletal rearrangements in more than 90% of injected cells with similar kinetics (time points ranging from 1 h to 12 h after injection) and at similar concentrations of injected plasmid (down to 0.2 ng/ μ l). Examination of Swiss 3T3 cells 1 h after their microinjection with a construct encoding V12 RAS (pEXV3 V12 RAS) revealed only lamellipodial actin rearrangement (Fig. 2B, small arrows) consistent with the involvement of Rac as a key downstream target of RAS signaling (14).

G2A Induced Stress Fiber Assembly Requires RhoA. Microinjection of constitutively active mutants of RhoA into Swiss 3T3 fibroblasts induces the formation of actin stress fibers and focal adhesion complexes (15). In addition, RhoA functions as a downstream component of signaling pathways initiated by ligand stimulation of the G protein-coupled lysophosphatidic acid receptor, leading to stress fiber assembly (16). To assess the requirement for RhoA activity in the induction of stress fibers by G2A, a construct encoding a MYC epitope-tagged dominant negative mutant form of RhoA (pEXV3 N19 RhoA) was coinjected with pEXV3 G2A into Swiss 3T3 cells. Coex-

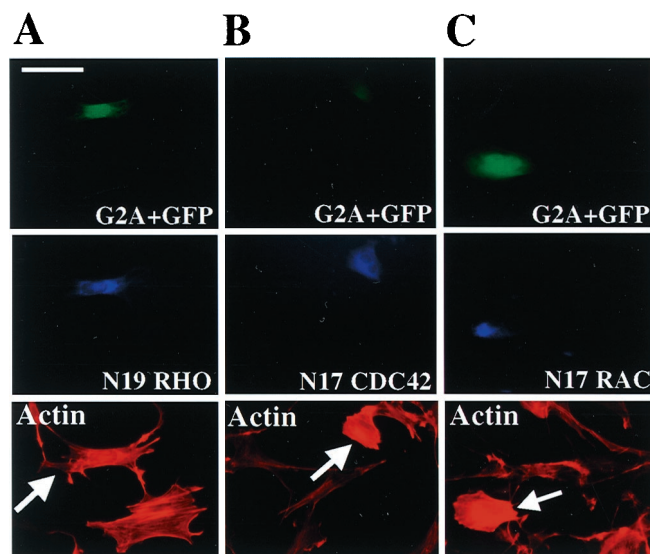


Fig. 3. Induction of stress fiber assembly by G2A is inhibited by N19 RhoA. Serum-starved Swiss 3T3 cells were microinjected with pEXV3 G2A and pEXV3 GFP plasmids together with pEXV3 constructs encoding (A) MYC epitope-tagged N19 RhoA, (B) MYC epitope-tagged N17 CDC42, or (C) MYC epitope-tagged N17 Rac1. Cells were fixed 4 h later and stained with 9E10 mAb to detect expression of dominant negative Rho family mutants (Middle) and rhodamine-conjugated phalloidin (Bottom). Large arrows indicate injected cells. (Bar = 50 μ m.)

pression of N19 RhoA inhibits G2A-mediated stress fiber induction, with injected and noninjected cells demonstrating indistinguishable cytoskeletal organization (Fig. 3A). This demonstrates that RhoA signaling is required for the induction of stress fiber assembly by G2A.

Induction of stress fiber assembly by G2A may be mediated by the sequential activation of CDC42, Rac, and Rho (17). To directly address the requirement for CDC42 and Rac activity, a construct encoding either a MYC epitope-tagged dominant negative mutant of CDC42 or Rac (pEXV3 N17 CDC42 or pEXV3 N17 Rac) was coinjected with pEXV3 G2A. Expression of N17 CDC42 or N17 Rac did not inhibit the assembly of stress fibers induced by G2A (Fig. 3B and C). Microinjection of pEXV3 N17 CDC42 or pEXV3 N17 Rac inhibited Bradykinin-induced formation of filopodia and platelet-derived growth factor induced lamellipodial extensions, respectively in over 80% of injected cells (data not shown).

G2A Activates SRF-Dependent Transcriptional Activation via RhoA. In addition to their effects on the actin cytoskeleton, Rho family GTPases regulate transcriptional events. RhoA has been shown to activate the transcription factor SRF (18), which cooperates with ternary complex factors in activating transcription at serum response elements within the promoters of growth factor-regulated genes such as *c-fos* (19). We performed transient transcriptional reporter assays in NIH 3T3 cells in which a G2A-encoding construct was cotransfected with a reporter construct comprising the firefly luciferase (Luc) gene driven by SRF-responsive sequences (SRF-Luc) (18). Normalization for variability in transfection efficiency was achieved by measuring the activity of a cotransfected thymidine kinase (TK) promoter-driven *Renilla* luciferase construct (pTK-*Renilla* Luciferase). Transient expression of G2A induces transcriptional activation of SRF-Luc, which is inhibited by coexpression of the Rho inhibitor C3 transferase (Fig. 4A).

G2A Activates RhoA. Limitations associated with the use of the dominant negative N19 RhoA mutant include its impact on

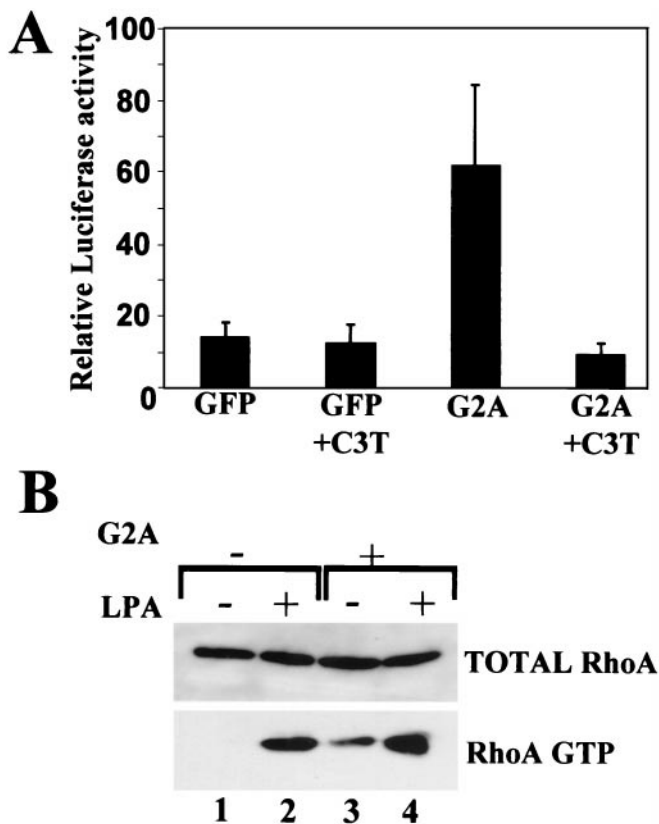


Fig. 4. (A) G2A induces transcriptional activation of SRF. NIH 3T3 cells were cotransfected with reporter plasmid pSRF-Luc, pTK-*Renilla* Luc, and pEXV3 G2A or pEXV3 GFP with or without pRK5 mycC3T (totaling 0.9 μ g DNA). Twenty four hours after transfection, cells were lysed and subjected to luciferase assays. Transfections and SRF-Luc assays were performed in triplicate, and results presented are typical of three independent experiments. (B) G2A activates RhoA in Swiss 3T3 cells. Swiss 3T3 cells were infected with MSCV GFP or MSCV G2AiresGFP retroviruses and 24 h later were serum-starved for 12 h. Cells subsequently were lysed, and lysates were incubated on ice for 1 h with glutathione *S*-transferase-RRBD immobilized on glutathione-agarose beads to affinity precipitate RhoA-GTP. Affinity precipitates (RhoA GTP) and aliquots of total lysates (total RhoA) were Western blotted with a mAb against RhoA. Lanes 2 and 4, lysophosphatidic acid (LPA) (1 μ g/ml, 5 min) stimulated activation of RhoA. Lanes 1 and 3, Increased levels of RhoA GTP in G2A expressing Swiss 3T3 cells compared with control Swiss 3T3 cells.

normal cytoskeletal integrity, irrespective of the presence or absence of a stimulating factor. We therefore used a direct biochemical approach to assay the activity of RhoA in cellular lysates obtained from Swiss 3T3 cells 36 h after their infection with murine stem cell virus (MSCV) GFP or MSCV G2AiresGFP retroviruses. Briefly, lysates were incubated with a glutathione *S*-transferase (GST) fusion protein containing the RhoA-GTP binding domain of the RhoA effector rhotekin (GST-RRBD) to affinity precipitate active GTP-bound RhoA as described (20). Cell populations were more than 90% GFP positive by FACS analysis before lysis. We observe elevated levels of RhoA-GTP in Swiss 3T3 cells infected with MSCV G2AiresGFP compared with that in cells infected with control MSCV GFP retroviruses (Fig. 4B, lanes 1 and 3). As a control, incubation with 1 μ g/ml lysophosphatidic acid for 5 min stimulated an increase in RhoA-GTP levels in both cell populations (Fig. 4B, lanes 2 and 4). In conclusion, although G2A may signal through several distinct effectors, we have identified RhoA activation leading to cytoskeletal rearrangement as a pathway downstream of G2A.

Induction of Rho-Dependent Cytoskeletal Rearrangement by G2A Is Mediated by $G\alpha 13$.

One route from GPCRs to RhoA is via members of the $G\alpha 12$ class of G proteins, including the ubiquitously expressed $G\alpha 12$ and $G\alpha 13$ (21), as well as $G\alpha q$ (22). Indeed, microinjection of constitutively active GTPase-deficient mutants of $G\alpha 12$ or $G\alpha 13$ subunits into Swiss 3T3 cells induces stress fiber assembly (13). More recently, the RGS domain containing p115 guanine nucleotide exchange factor (p115 GEF) has been shown to mediate RhoA activation by the $G\alpha 12$ class of G proteins (23).

We used MEFs derived from various $G\alpha$ -deficient mice to genetically test the involvement of specific G proteins in the induction of Rho-dependent stress fiber assembly by G2A. Microinjection of pEXV3 G2A.GFP into wild-type, $G\alpha q/11$ KO, and $G\alpha 12$ KO MEFs elicited stress fiber assembly with identical frequency and kinetics. However, $G\alpha 13$ KO and $G\alpha 12/G\alpha 13$ KO MEFs did not accumulate abundant stress fibers in response to microinjection (Fig. 5), demonstrating that G2A activation of RhoA-dependent actin rearrangement requires $G\alpha 13$, not $G\alpha 12$ or $G\alpha q$.

To exclude the possibility that the unresponsiveness of $G\alpha 13$ KO MEFs to G2A is caused by secondary mutations or epigenetic changes other than ablation of $G\alpha 13$ function, $G\alpha 13$ -deficient fibroblasts were reconstituted with functional $G\alpha 13$ by

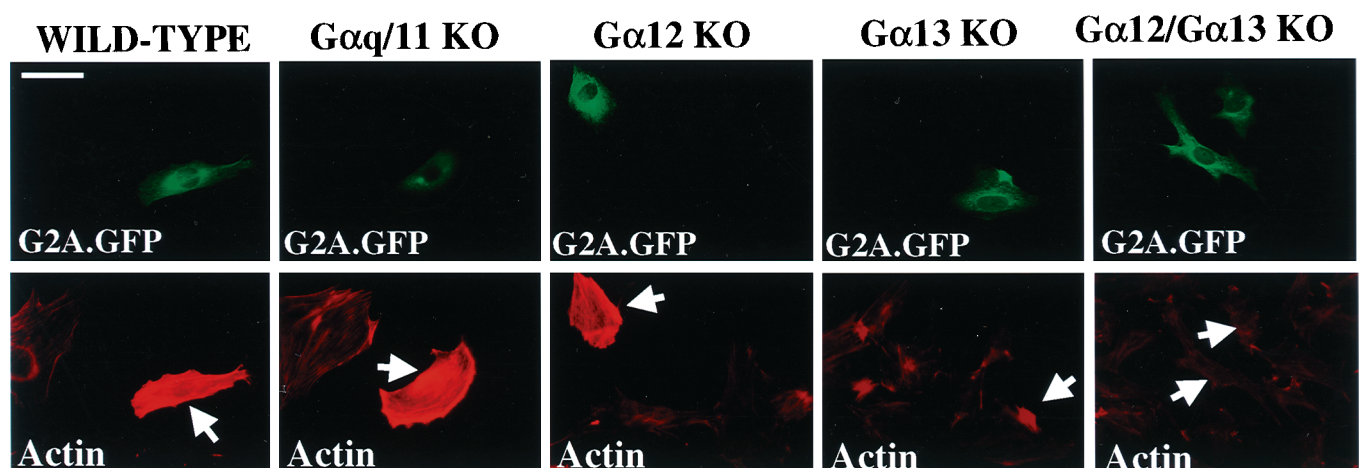


Fig. 5. G2A-induced stress fiber assembly requires $G\alpha 13$. The indicated MEFs were microinjected with pEXV3 G2A.GFP, fixed 4 h later, and stained with rhodamine-conjugated phalloidin. (Upper) GFP fluorescence. (Lower) Phalloidin-stained actin. Arrows indicate injected cells. (Bar = 50 μ m.)

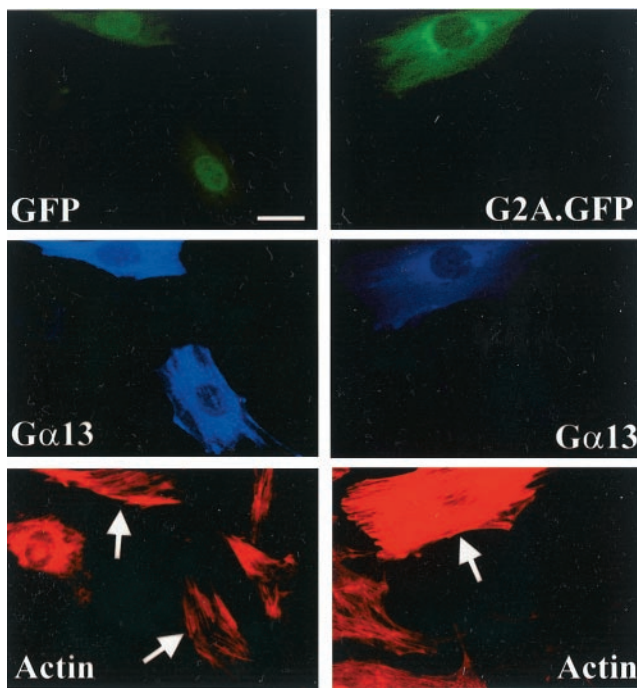


Fig. 6. Reconstitution of functional $G\alpha 13$ in $G\alpha 13$ KO MEFs restores their responsiveness to G2A. $G\alpha 13$ KO MEFs were microinjected with pEXV3 GFP or pEXV3 G2A.GFP together with pCIS $G\alpha 13$, fixed 4 h later, and stained with rhodamine-conjugated phalloidin (*Bottom*), and rabbit antiserum against $G\alpha 13$ to detect ectopically expressed $G\alpha 13$ (*Middle*). (*Upper*) GFP fluorescence. Arrows indicate injected cells. (Bar = 20 μm .)

coinjecting a construct encoding $G\alpha 13$ (pCIS $G\alpha 13$). Whereas microinjection of pCIS $G\alpha 13$ alone into $G\alpha 13$ KO MEFs did not elicit stress fiber assembly (Fig. 6 *Left*), coinjection of pCIS $G\alpha 13$ with pEXV3 G2A.GFP induced the formation of abundant actin stress fibers (Fig. 6 *Right*). Identical results were obtained with $G\alpha 12/G\alpha 13$ KO MEFs (data not shown).

We conclude that G2A couples to $G\alpha 13$, through which G2A mediates activation of RhoA, leading to cytoskeletal reorganization and transcriptional activation of SRF.

Discussion

Transcriptional induction of G2A in response to diverse proliferative and genotoxic stimuli together with the impact of its ectopic expression on cell-cycle progression through G_2/M suggested a possible role of this orphan GPCR in negative regulatory checkpoint mechanisms in lymphocytes. We now have extended our studies and demonstrate a direct signaling pathway from G2A leading to RhoA via $G\alpha 13$. It recently was reported that cytoskeletal and morphological alterations induced by G2A expression in fibroblasts are similar to those induced by activated mutants of RhoA, $G\alpha 12$, or $G\alpha 13$ (24). By assaying levels of RhoA-GTP in G2A-expressing cells, we have directly demonstrated activation of RhoA. The role of $G\alpha 13$ is established by its requirement for RhoA-dependent cytoskeletal responses to G2A expression in $G\alpha 13$ KO MEFs.

Interestingly, a large proportion of the G2A.GFP fusion protein is localized to the cytoplasm, with a pronounced perinuclear pattern suggesting its presence in the endosomal compartment. Although this could simply be the result of its overexpression, the localization pattern of G2A.GFP is similar to that of an analogous β_2 adrenergic receptor GFP fusion protein ($\beta_2\text{AR-GFP}$) after agonist stimulation (25). It is possible, therefore, that G2A is constitutively active when expressed in heterologous cell types, binds a ligand that is produced intracellularly, or is a ligand

independent receptor subject to continual down-regulatory modification and internalization. The possibility that a ligand for G2A may be a small bioactive molecule is strengthened by certain conserved features shared by G2A and other GPCRs with this ligand specificity (26).

The well-documented morphological alterations induced in fibroblasts expressing constitutively activated mutants of RhoA or $G\alpha 13$ (27, 28) suggests that deregulation of RhoA activity by G2A is responsible for its impact on cellular morphology. A role for RhoA in proliferative control also has been demonstrated in fibroblasts in the context of oncogenic and mitogenic stimulation (29–31). Although we do not observe any significant effects of G2A expression on $G_1 \rightarrow S$ cell-cycle progression of quiescent fibroblasts after serum stimulation or in G_1 -arrested fibroblasts after removal of a thymidine-induced block (J.H.S.K., L.Q.L., and O.N.W., unpublished observations), G2A expression promotes their survival and proliferation in confluent cultures by overriding contact inhibition of growth.

G2A induces morphological transformation of NIH 3T3 fibroblasts yet inhibits transformation of RAT1 fibroblasts to anchorage independence by BCR-ABL (6). Although these observations could be reconciled by use of different fibroblastic lines, G2A also transforms RAT1 fibroblasts to anchorage independent growth, albeit at a much lower frequency compared with BCR-ABL (data not shown). It is possible, therefore, that BCR-ABL and G2A signals in combination may elicit a different biological outcome to that induced by each in isolation. In this regard, RAC is implicated as a downstream target of BCR-ABL (32), and concurrent deregulation of both RAC and RhoA GTPases may be incompatible with viability or proliferation (33). This phenomenon also could underlie the suppressive effect of G2A on B lymphoid transformation by BCR-ABL in long-term bone marrow cultures, which depend on stromal contact to sustain B lymphopoiesis.

Inhibition of B lymphoid transformation is the only property so far ascribed to G2A in a cell type within which it is actually expressed. Further biological characterization of G2A in lymphoid cells is of primary importance, and we have generated G2A-deficient mice with this objective in mind. A reduction in latency for leukemogenesis in mice transplanted with BCR-ABL-infected bone marrow cells from these animals confirms our previous observations. In addition, a role for G2A in the regulation of T lymphocyte proliferation has been revealed in our studies of G2A-deficient mice (L.Q.L., J.H.S.K., and O.N.W., unpublished observations). In T lymphocytes, RhoA is implicated in the regulation of T cell antigen receptor (TCR)/cytoskeleton interaction and sustained TCR-dependent signaling (34, 35). G2A therefore may play a role in the regulation of TCR-dependent cytoskeletal rearrangement. For example, G2A may function in the maintenance of the immunological synapse after antigen receptor/MHC-peptide interaction during which segregation of integrin and antigen receptors into specific areas at cell/cell contacts precedes their reorganization via cytoskeletal mechanisms into clusters mediating sustained signaling (36).

We thank Jamie White and Shirley Quan for assistance in the preparation of this manuscript, Dr. James Feramisco (University of California, San Diego) for helpful discussions, critical review of the manuscript, and use of the microinjection facility, and Brian Smith and Matt Zimmerman for their help and advice with microinjection. We also thank Drs. Richard Waldren and Lutz Birnbaumer for critical review of the manuscript. O.N.W. is an Investigator of the Howard Hughes Medical Institute, J.H.S.K. is a Fellow of the Leukemia and Lymphoma Society, and L.Q.L. is supported by a National Institutes of Health training grant (5-T32-CA009120–25). These studies were supported by National Cancer Institute Grant CA76204 to O.N.W. and National Institutes of Health Grant GM34236 to M.I.S.

1. Hedin, K. E., Duerson, K. & Clapham, D. E. (1993) *Cell Signal* **5**, 505–518.
2. Offermanns, S., Schultz, G. & Rosenthal, W. (1991) *Methods Enzymol.* **195**, 286–301.
3. Luttrell, L. M., Ferguson, S. S., Daaka, Y., Miller, W. E., Maudsley, S., Della Rocca, G. J., Lin, F., Kawakatsu, H., Owada, K., Luttrell, D. K., *et al.* (1999) *Science* **283**, 655–661.
4. Beadling, C., Druey, K. M., Richter, G., Kehrl, J. H. & Smith, K. A. (1999) *J. Immunol.* **162**, 2677–2682.
5. Fraser, C. M. (1995) *J. Nucl. Med.* **36**, 17S–21S.
6. Weng, Z., Fluckiger, A. C., Nisitani, S., Wahl, M. I., Le, L. Q., Hunter, C. A., Fernal, A. A., Le Beau, M. M. & Witte, O. N. (1998) *Proc. Natl. Acad. Sci. USA* **95**, 12334–12339.
7. Choi, J. W., Lee, S. Y. & Choi, Y. (1996) *Cell. Immunol.* **168**, 78–84.
8. Kyaw, H., Zeng, Z., Su, K., Fan, P., Shell, B. K., Carter, K. C. & Li, Y. (1998) *DNA Cell Biol* **17**, 493–500.
9. Offermanns, S., Mancino, V., Revel, J.-P. & Simon, M. I. (1997) *Science* **275**, 533–536.
10. Offermanns, S., Toombs, C. F., Hu, Y.-H. & Simon, M. I. (1997) *Nature (London)* **389**, 183–186.
11. Boguski, M. & McCormick, F. (1993) *Nature (London)* **366**, 643–654.
12. Giancotti, F. G. & Ruoslahti, E. (1999) *Science* **285**, 1028–1032.
13. Gohla, A., Harhammer, R. & Schultz, G. (1998) *J. Biol. Chem.* **273**, 4653–4659.
14. Scita, G., Nordstrom, J., Carbone, R., Tenca, P., Giardina, G., Gutkind, S., Bjarnegard, M., Betsholtz, C. & Di Fiore, P. P. (1999) *Nature (London)* **401**, 290–293.
15. Ridley, A. J. & Hall, A. (1992) *Cell* **70**, 389–399.
16. Barry, S. T. & Critchley, D. R. (1994) *J. Cell Sci.* **107**, 2033–2045.
17. Nobes, C. D. & Hall, A. (1995) *Cell* **81**, 53–62.
18. Hill, C. S., Wynne, J. & Treisman, R. (1995) *Cell* **81**, 1159–1170.
19. Marais, R., Wynne, J. & Treisman, R. (1993) *Cell* **73**, 381–393.
20. Ren, X. D., Kiousses, W. B. & Schwartz, M. A. (1999) *EMBO J.* **18**, 578–585.
21. Strathmann, M. P. & Simon, M. I. (1991) *Proc. Natl. Acad. Sci. USA* **88**, 5582–5586.
22. Mao, J., Yuan, H., Xie, W., Simon, M. I. & Wu, D. (1998) *J. Biol. Chem.* **273**, 27118–27123.
23. Hart, M. J., Jiang, X., Kozasa, T., Roscoe, W., Singer, W. D., Gilman, A. G., Sternweis, P. C. & Bollag, G. (1998) *Science* **280**, 2112–2114.
24. Zohn, I. E., Klinger, M., Karp, X., Kirk, H., Symons, M., Chrzanowska-Wodnicka, M., Der, C. J. & Kay, R. J. (2000) *Oncogene* **19**, 3866–3877.
25. Kallal, L. & Benovic, J. L. (2000) *Trends Pharmacol. Sci.* **21**, 175–180.
26. Dohlman, H. G., Thorner, J., Caron, M. G. & Lefkowitz, R. J. (2000) *Annu. Rev. Biochem.* **60**, 653–688.
27. Khosravi-Far, R., Solski, P., Clark, G. J., Kinch, M. J. & Der, C. J. (1995) *Mol. Cell. Biol.* **15**, 6443–6453.
28. Vara Prasad, M., Shore, S. K. & Dhanasekaran, N. (1994) *Oncogene* **9**, 2425–2429.
29. Qiu, R.-G., Chen, J., McCormick, F. & Symons, M. (1995) *Proc. Natl. Acad. Sci. USA* **92**, 11781–11785.
30. Olson, M. F., Ashworth, A. & Hall, A. (1995) *Science* **269**, 1270–1272.
31. Olson, M. F., Paterson, H. F. & Marshall, C. J. (1998) *Nature (London)* **394**, 295–299.
32. Skorski, T., Wlodarski, P., Daheron, L., Salomoni, P., Nieborowska-Skorska, M., Majewski, M., Wasik, M. & Calabretta, B. (1998) *Proc. Natl. Acad. Sci. USA* **95**, 11858–11862.
33. Sander, E. E., ten Klooster, J. P., van Delft, S., van der Kammen, R. A. & Collard, J. G. (1999) *J. Cell Biol.* **147**, 1009–1022.
34. Caplan, S. & Baniyash, M. (2000) *Immunol. Today* **21**, 223–228.
35. Angkathachai, V. & Finkel, T. H. (1999) *J. Immunol.* **163**, 3819–3825.
36. Grakoui, A., Bromley, S. K., Sumen, C., Davis, M. M., Shaw, A. S., Allen, P. M. & Dustin, M. L. (1999) *Science* **285**, 221–227.